

PAPER • OPEN ACCESS

Classical echoes of quantum boundary conditions



To cite this article: Giuliano Angelone *et al* 2024 *J. Phys. A: Math. Theor.* **57** 425304

View the [article online](#) for updates and enhancements.

You may also like

- [New cluster algebras from old: integrability beyond Zamolodchikov periodicity](#)
Andrew N W Hone, Wookyung Kim and Takafumi Mase
- [Entropic uncertainty relations and entanglement detection from quantum designs](#)
Yundu Zhao, Shan Huang and Shengjun Wu
- [Generalized hydrodynamics for the volterra lattice: ballistic and non-ballistic behavior of correlation functions](#)
Guido Mazzuca

Classical echoes of quantum boundary conditions

Giuliano Angelone^{1,2,*} , Paolo Facchi^{1,2} 
and Marilena Ligabò³

¹ Dipartimento di Fisica, Università degli Studi di Bari, I-70126 Bari, Italy

² INFN, Sezione di Bari, I-70126 Bari, Italy

³ Dipartimento di Matematica, Università degli Studi di Bari, I-70125 Bari, Italy

E-mail: giuliano.angelone@uniroma1.it, paolo.facchi@ba.infn.it
and marilena.ligabo@uniba.it

Received 3 May 2024; revised 28 June 2024

Accepted for publication 27 August 2024

Published 4 October 2024



CrossMark

Abstract

We consider a non-relativistic particle in a one-dimensional box with all possible quantum boundary conditions that make the kinetic-energy operator self-adjoint. We determine the Wigner functions of the corresponding eigenfunctions and analyze in detail their classical limit, governed by their behavior in the high-energy regime. We show that the quantum boundary conditions split into two classes: all local and regular boundary conditions collapse to the same classical boundary condition, while a dependence on singular non-local boundary conditions persists in the classical limit.

Keywords: classical limit, Wigner function, particle in a box, quantum boundary conditions, self-adjoint extensions

1. Introduction

The phase-space formulation of quantum mechanics allows to represent states and operators as functions on classical phase-space [1]. It has various applications, ranging from quantum optics, quantum chaos and quantum computing to classical optics and signal analysis [2, 3]. In quantum physics, phase-space methods have also been used to characterize the non-classicality of quantum states, to identify and reconstruct states via quantum tomography, and to understand the quantum-to-classical transition and the correspondence principle [4–7].

* Author to whom any correspondence should be addressed.



Original Content from this work may be used under the terms of the [Creative Commons Attribution 4.0 licence](https://creativecommons.org/licenses/by/4.0/). Any further distribution of this work must maintain attribution to the author(s) and the title of the work, journal citation and DOI.

Between many possible quantum (quasi-)probability distributions, the Wigner function arguably gives the most natural phase-space representation of quantum mechanics. In spite of a long history of research, the theory of Wigner functions for systems on a manifold (or phase-space) with non-trivial topology, as well as having boundaries, is still not complete. For example, group-theoretical approaches have recently been applied for the Wigner function on the cylinder $\mathbb{S}^1 \times \mathbb{R}$ [8, 9], the discrete cylinder $\mathbb{Z} \times \mathbb{R}$ [10, 11] and the torus $\mathbb{S}^1 \times \mathbb{S}^1$ [12], whereas the deformation quantization approach is usually employed for manifold with boundaries, see e.g. [13–16].

In this paper, we are interested in two related subjects: (i) the study of the Wigner function for eigenfunctions of the kinetic-energy operator (i.e. the free Hamiltonian) acting in a one-dimensional box with general self-adjoint boundary conditions, and (ii) the analysis of these Wigner functions in the classical limit, that is in the high-energy regime. Preliminary results in this direction have already been obtained: the Wigner function has been studied in [17, 18] for the one-dimensional box with Dirichlet boundary conditions, and in [19, 20] for the half-line with Robin boundary conditions. Besides, in [21–23] the classical limit of the position and momentum probability distributions for the one-dimensional box with Dirichlet boundary conditions have been investigated.

The paper is organized as follows. After introducing in section 2 the free Hamiltonian with general self-adjoint boundary conditions, in section 3 we explicitly compute the Wigner functions associated with the eigenfunctions of the Hamiltonian, and describe how to determine their classical limit. In section 4, then, we classify the possible classical limits by analyzing the asymptotic properties of the spectrum in the high-energy regime. Finally, in section 5 we discuss the results and compare the classical limits with corresponding classical probability distributions.

2. A quantum particle in a box

We consider a quantum particle of mass m , confined in a one-dimensional box of unit length, namely the interval $J = [-1/2, 1/2]$. This system is formally described by the kinetic-energy operator,

$$H = -\frac{\hbar^2}{2m} \frac{d^2}{dx^2}, \quad (1)$$

which acts on a proper subspace of the Hilbert space $L^2(J)$. As it is well-known, see e.g. [24, 25], equation (1) prescribes the action of H only in the *bulk* of the system. The Hamiltonian H should indeed be equipped with suitable boundary conditions (BCs), specifying the behavior of the particle at the boundary of the interval, in order to generate a well-defined quantum dynamics. In quantum mechanics the possible BCs, encoded in the domain $\mathcal{D}(H)$ of H , cannot be arbitrary, but are constrained by the requirement that H must be a *self-adjoint* operator, i.e. $\mathcal{D}(H) = \mathcal{D}(H^*)$ and $H = H^*$. Indeed, self-adjointness is a necessary and sufficient condition for a (Hermitian) operator to have a purely real spectrum and to generate a unitary dynamics.

Different domains correspond to different behaviors of the particle at the boundary, give rise to different dynamics and represent different physical situations. All the self-adjoint realizations of the operator (1) are known to be in one-to-one correspondence with the set of 2×2 unitary matrices $U \in \text{U}(2)$ [26–29]. Each of these realizations, which we henceforth denote by H_U , is defined on the domain

$$\mathcal{D}(H_U) = \{ \psi \in \mathcal{H}^2(J) : (I - U)\Psi' = i(I + U)\Psi \}, \quad U \in \text{U}(2), \quad (2)$$

where $\mathcal{H}^2(J)$ is the space of wave functions ψ with square-integrable first and second derivative, ψ' and ψ'' , on the interval $J = [-1/2, 1/2]$, while the \mathbb{C}^2 vectors

$$\Psi := \begin{pmatrix} \psi(-\frac{1}{2}) \\ \psi(\frac{1}{2}) \end{pmatrix}, \quad \Psi' := \begin{pmatrix} -\psi'(-\frac{1}{2}) \\ \psi'(\frac{1}{2}) \end{pmatrix}, \quad (3)$$

contain respectively the boundary values of ψ and of its normal derivative, so that the constraint⁴

$$(I - U)\Psi' = i(I + U)\Psi, \quad (4)$$

compactly encodes the BCs to be satisfied by the wave function at the endpoints of the box $x = \pm 1/2$. Some physical properties of the BCs will be highlighted in section (2.1).

Let us now introduce the Wigner function associated with a wave function $\psi \in L^2(\mathbb{R})$, [1–3, 30]. The Wigner function $W\psi$ represents the joint quasi-probability distribution of position and momentum in the state ψ and it is given by

$$W\psi(x, p) := \frac{1}{2\pi\hbar} \int_{\mathbb{R}} e^{-ipy/\hbar} \psi(x + \frac{y}{2}) \overline{\psi(x - \frac{y}{2})} dy \quad (5)$$

where $(x, p) \in \mathbb{R}^2$. For a wave function ψ spatially confined in the interval J , i.e. for an element of $L^2(J)$, the associated Wigner function of ψ can be computed considering the function defined on \mathbb{R} that coincides with ψ in the interval J and vanishes outside. With this procedure one obtains

$$W\psi(x, p) = \frac{1}{2\pi\hbar} \int_{\mathbb{R}} e^{-ipy/\hbar} \psi(x + \frac{y}{2}) \overline{\psi(x - \frac{y}{2})} dy \quad (6a)$$

$$= \frac{\chi(x)}{2\pi\hbar} \int_{2|x|-1}^{1-2|x|} e^{-ipy/\hbar} \psi(x + \frac{y}{2}) \overline{\psi(x - \frac{y}{2})} dy, \quad (6b)$$

where χ is the characteristic function of the interval $J = [-1/2, 1/2]$, i.e. $\chi(x) = 1$ if $|x| \leq 1/2$ and $\chi(x) = 0$ if $|x| > 1/2$, see figure 1. We stress that, although being defined for $(x, p) \in \mathbb{R}^2$, by construction the above Wigner function vanishes for $|x| > 1/2$, i.e. outside of the box⁵.

In the following we are interested both in the explicit expression of the Wigner function for an eigenfunction of H_U , which will be the main topic of section 3, and in its behavior in the *classical limit*, which we will discuss in section 4. Before moving on, however, we spend a few words on the allowed quantum BCs, giving some examples in section 2.1 and introducing a useful parametrization of $\text{U}(2)$ in section 2.2.

⁴ In some related works, as e.g. [26–28], the alternative parametrization $(I + \tilde{U})\Psi' = -i(I - \tilde{U})\Psi$ is adopted, with a given $\tilde{U} \in \text{U}(2)$; here, following [29, 31], we find convenient to put $\tilde{U} = -U^\dagger$.

⁵ Interestingly, equation (6) can also be obtained by applying a ‘regularization’ procedure: in [32], e.g. a particle moving freely on the half-line is treated as moving on the full line in the presence of an infinite potential wall, the latter being realized as a limit of a smooth (Morse) potential.

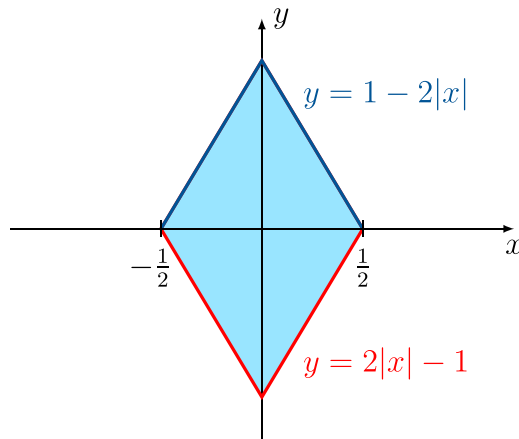


Figure 1. Integration region of equation (6) (shaded area): as x varies in $J = [-1/2, 1/2]$ the integrand function contributes to the integral only for $-1/2 \leq x + y/2 \leq 1/2$ and $-1/2 \leq x - y/2 \leq 1/2$, that is for $2|x| - 1 \leq y \leq 1 - 2|x|$.

2.1. Topology of quantum boundary conditions

If the matrix $I - U$ is invertible, the BC in equation (4) can also be expressed as

$$\Psi' = M_U \Psi, \quad M_U = i(I + U)(I - U)^{-1}, \tag{7}$$

where M_U , being the inverse Cayley transform of U , is an Hermitian matrix. For a more general inversion formula, holding also when $I - U$ is not invertible, see e.g. equation (19) of [31]. Two interesting families of BCs are given respectively by (symmetric) Robin conditions

$$U_R(\alpha) := e^{i\alpha} I, \quad \Psi' = -\cot\left(\frac{\alpha}{2}\right) \Psi, \tag{8}$$

with $\alpha \in [0, 2\pi)$, that reduce to Dirichlet ($\Psi = 0$) and Neumann ($\Psi' = 0$) BCs respectively for $\alpha = 0$ and $\alpha = \pi$, and by pseudo-periodic BCs

$$U_{pp}(\alpha) := -\begin{pmatrix} 0 & e^{-i\alpha} \\ e^{i\alpha} & 0 \end{pmatrix}, \quad \begin{cases} \psi\left(\frac{1}{2}\right) = e^{i\alpha} \psi\left(-\frac{1}{2}\right) \\ \psi'\left(\frac{1}{2}\right) = e^{i\alpha} \psi'\left(-\frac{1}{2}\right) \end{cases}, \tag{9}$$

with $\alpha \in [0, 2\pi)$, that in turn reduce to periodic and anti-periodic conditions when $\alpha = 0$ and $\alpha = \pi$, respectively.

As the reader may have noticed, BCs can be either local or non-local: Robin BCs, e.g. are local, as they do not mix the boundary values of ψ at the left edge $x = -1/2$ with those at the right edge $x = 1/2$, whereas pseudo-periodic BCs are non-local. Differently from local BCs, which physically confine the particle inside a box, non-local BCs are actually related to the physics of a particle in a ring. Arbitrary BCs can be effectively realized in a ring with a junction, depicted in figure 2. In this model, the matrix U encodes the physical properties of the junction. In particular, local BCs are associated with an impermeable barrier that ‘decouples’ the left edge from the right one, while non-local BCs permit the particle to cross the junction. The locality of the BCs can be quantified by looking at the probability current density

$$j_\psi(x) := -\frac{\hbar^2}{2m} \left(\overline{\psi'(x)}\psi(x) - \overline{\psi(x)}\psi'(x) \right) \tag{10}$$

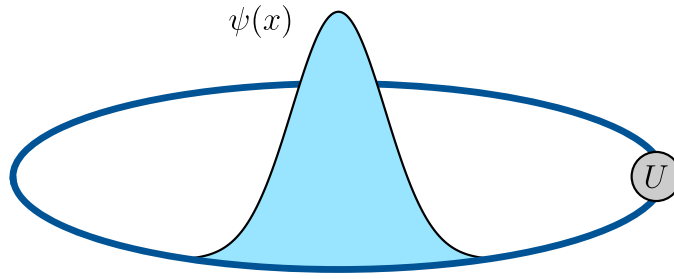


Figure 2. A quantum particle in a ring with a junction.

associated with a wave function $\psi(x)$: local BCs, forbidding the transmission across the junction, are indeed characterized by a vanishing current at the endpoints of the ring, that is by $j_\psi(-1/2) = j_\psi(1/2) = 0$. For non-local BCs, instead, the current density does not generally vanishes at the endpoints but the outgoing and incoming currents are exactly balanced, namely $j_\psi(-1/2) = j_\psi(1/2)$, in accordance with the unitarity of the evolution and the conservation of probability ensured by the self-adjointness of the Hamiltonian.

We also mention that the BCs in equations (4)–(29), upon substituting $\pm 1/2 \rightarrow 0^\mp$, are substantially the same that one finds by considering the scattering of a one-dimensional particle with a generalized point defect located at (say) the origin of the system, that is by studying the self-adjoint extensions of the free Hamiltonian (1) for a particle living in the punctured line $\mathbb{R} \setminus \{0\} = \mathbb{R}_- \cup \mathbb{R}_+$, see e.g. [33–36]. In this case, local BCs are usually denoted as confining (or separated), as they describe an impenetrable barrier effectively isolating the \mathbb{R}_- region from the \mathbb{R}_+ region, whereas non-local BCs are non-confining and allow the transmission of the particle between the two regions. Remarkably, for this system it is also possible to find an explicit expression of the transmission and reflection coefficients in terms of an arbitrary BC $U \in U(2)$, see e.g. [37, 38].

More generally, let us stress that BCs are often crucial to determine the spatial topology of a quantum system. We refer the reader to e.g. [26, 28, 39–44] for further details.

2.2. Parametrization of the quantum boundary conditions

All the unitary matrices in $U(2)$ can be parametrized by using five real parameters [45]:

$$e^{i\eta} \begin{pmatrix} m_0 + im_3 & m_2 + im_1 \\ -m_2 + im_1 & m_0 - im_3 \end{pmatrix}, \quad (11)$$

with $\eta \in [0, 2\pi)$, and $m_0, m_1, m_2, m_3 \in \mathbb{R}$ such that

$$m_0^2 + m_1^2 + m_2^2 + m_3^2 = 1. \quad (12)$$

In order to obtain a one-to-one parametrization of $U(2)$, the values $(\eta, m_0, m_1, m_2, m_3)$ and $(\eta + \pi, -m_0, -m_1, -m_2, -m_3)$ have to be identified, as they give the same matrix:

$$e^{i\eta} \begin{pmatrix} m_0 + im_3 & m_2 + im_1 \\ -m_2 + im_1 & m_0 - im_3 \end{pmatrix} = e^{i(\eta+\pi)} \begin{pmatrix} -m_0 - im_3 & -m_2 - im_1 \\ m_2 - im_1 & -m_0 + im_3 \end{pmatrix}. \quad (13)$$

To achieve this, we henceforth restrict $\eta \in [0, \pi)$. On the other hand, equation (12) tells us that only four parameters are actually independent and, since the pair (m_0, m_1) always takes values

in the unit disk $D = \{(x, y) \in \mathbb{R}^2 : x^2 + y^2 \leq 1\}$, it is convenient to express m_2 and m_3 in terms of a new parameter $\beta \in [0, 2\pi)$:

$$m_2 = \sqrt{1 - m_0^2 - m_1^2} \cos(\beta), \quad m_3 = \sqrt{1 - m_0^2 - m_1^2} \sin(\beta). \tag{14}$$

Therefore we have that

$$U(2) = \{U(\eta, m_0, m_1, \beta) : \eta \in [0, \pi), (m_0, m_1) \in D, \beta \in [0, 2\pi)\}, \tag{15}$$

where for all $\eta \in [0, \pi)$, $(m_0, m_1) \in D$ and $\beta \in [0, 2\pi)$:

$$U(\eta, m_0, m_1, \beta) := e^{i\eta} \begin{pmatrix} m_0 + i\sqrt{1 - m_0^2 - m_1^2} \sin(\beta) & \sqrt{1 - m_0^2 - m_1^2} \cos(\beta) + im_1 \\ -\sqrt{1 - m_0^2 - m_1^2} \cos(\beta) + im_1 & m_0 - i\sqrt{1 - m_0^2 - m_1^2} \sin(\beta) \end{pmatrix}. \tag{16}$$

Notice that if $m_0^2 + m_1^2 = 1$ then the matrix $U(\eta, m_0, m_1, \beta)$ does not depend on β , in that case we will fix $\beta = 0$.

Observe that Robin BCs (8) correspond to

$$U_R(\alpha) = \begin{cases} U(\alpha, 1, 0, 0), & \text{if } 0 \leq \alpha < \pi, \\ U(\alpha - \pi, -1, 0, 0), & \text{if } \pi \leq \alpha < 2\pi, \end{cases} \tag{17}$$

whereas pseudo-periodic BCs (9) correspond to

$$U_{pp}(\alpha) = \begin{cases} U(\frac{\pi}{2}, 0, \cos(\alpha), 0), & \text{if } 0 \leq \alpha < \pi, \\ U(\frac{\pi}{2}, 0, \cos(\alpha), \pi), & \text{if } \pi \leq \alpha < 2\pi. \end{cases} \tag{18}$$

The eigenvalues of $U(\eta, m_0, m_1, \beta)$ depend only on η and m_0 and are given by

$$\lambda_U^\pm := \exp i [\eta \pm \arccos(m_0)], \tag{19}$$

and in particular

$$\lambda_U^- = 1 \Leftrightarrow m_0 = \cos(\eta), \tag{20a}$$

$$\lambda_U^+ = 1 \Leftrightarrow \eta = -\arccos(m_0) = 0 \Leftrightarrow \eta = 0, \quad m_0 = 1. \tag{20b}$$

The above values are relevant since the inverse Cayley transform of $U(\eta, m_0, m_1, \beta)$ is singular whenever $I - U(\eta, m_0, m_1, \beta)$ is not invertible, that is when λ_U^- or λ_U^+ is equal to 1. Otherwise, it is the well defined Hermitian matrix

$$M_{U(\eta, m_0, m_1, \beta)} = \frac{1}{m_0 - \cos \eta} \begin{pmatrix} -\sin(\eta) + r \sin(\beta) & m_1 - i r \cos(\beta) \\ m_1 + i r \cos(\beta) & -\sin(\eta) - r \sin(\beta) \end{pmatrix}, \tag{21}$$

where $r = \sqrt{1 - m_0^2 - m_1^2}$. In figure 3, BCs having at least one eigenvalue equal to 1 are represented in the parameter space of (m_0, m_1) , for a given value of η . Note that, in particular, the Dirichlet condition $U_R(0) = I$ is the only one having $\lambda_U^- = \lambda_U^+ = 1$.

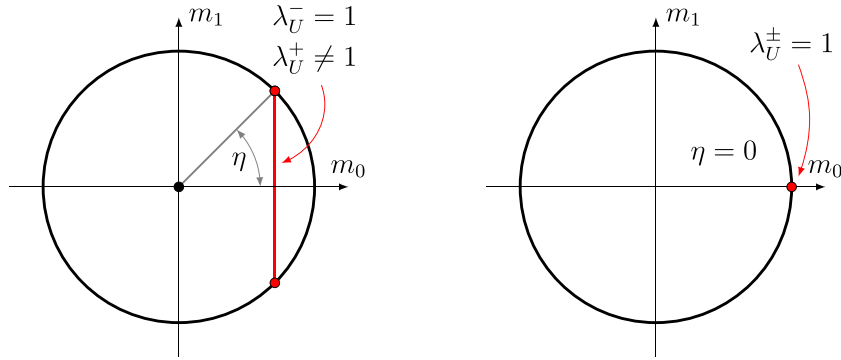


Figure 3. Boundary conditions $U(\eta, m_0, m_1, \beta)$ having at least one eigenvalue λ_U^\pm equal to 1 are shown, in red, in the parameter space $(m_0, m_1) \in D$, for $0 < \eta < \pi$ (left) and $\eta = 0$ (right).

Table 1. Some examples of BCs, and of the corresponding unitary matrices U , having different locality and regularity properties. We take $g \in \mathbb{R} \setminus \{0\}$ and $\alpha \in [0, 2\pi)$.

	Regular	Singular
Local	Symmetric Robin $\begin{pmatrix} e^{i\alpha} & 0 \\ 0 & e^{i\alpha} \end{pmatrix}$	Mixed Dirichlet-Neumann $\begin{pmatrix} -1 & 0 \\ 0 & 1 \end{pmatrix}$
Non-local	δ -interaction ($g \neq 0$) $\begin{pmatrix} \frac{g}{g-i} & \frac{i}{g-i} \\ \frac{i}{g-i} & \frac{g}{g-i} \end{pmatrix}$	Pseudo-periodic $-\begin{pmatrix} 0 & e^{-i\alpha} \\ e^{i\alpha} & 0 \end{pmatrix}$

For later convenience, we introduce the definition of *regular* and *singular* BCs. We say that the unitary matrix $U(\eta, m_0, m_1, \beta)$ (and the corresponding BC) is *singular* if the eigenvalues satisfy $\lambda_U^- = 1$ and $\lambda_U^+ \neq 1$, that is if

$$m_0 = \cos(\eta) \neq 1, \tag{22}$$

while it is *regular* otherwise. In other words the matrices in $U(2)$ having zero or two eigenvalues equal to 1 are regular, while the ones having just one eigenvalue 1 are singular. Besides, excluding the case of the identity matrix I (corresponding to the Dirichlet condition), which is regular by definition but does not admit the inverse Cayley transform, a generic unitary matrix U is regular if and only if it admits the inverse Cayley transform. Notice that the matrices corresponding to Robin BCs in equation (17) are regular (including the Dirichlet condition), while the matrices corresponding to pseudo-periodic BCs in equation (9) are singular. In general, however, BCs can be either regular or singular, independently of their locality. We give some interesting physical examples in table 1, where we also introduce the matrix

$$U_\delta(g) := \begin{pmatrix} \frac{g}{g-i} & \frac{i}{g-i} \\ \frac{i}{g-i} & \frac{g}{g-i} \end{pmatrix} \tag{23}$$

with $g \in \mathbb{R}$, implementing the so-called δ -interaction [33, 46], that is the BCs

$$\psi\left(\frac{1}{2}\right) = \psi\left(-\frac{1}{2}\right), \quad \psi'\left(-\frac{1}{2}\right) - \psi'\left(\frac{1}{2}\right) = 2g\psi\left(\frac{1}{2}\right). \quad (24)$$

These BCs are non-local for any $g \in \mathbb{R}$ and regular for $g \neq 0$, since the eigenvalues of $U_\delta(g)$ are 1 and $(g+i)/(g-i)$.

3. Wigner functions

In this section we explicitly determine the Wigner function of an eigenfunction of H_U , with $U = U(\eta, m_0, m_1, \beta) \in \mathbf{U}(2)$, $\eta \in [0, \pi)$, $(m_0, m_1) \in D$ and $\beta \in [0, 2\pi)$, that is a non-zero solution of the eigenvalue equation

$$H_U \psi = E \psi, \quad \psi \in \mathcal{D}(H_U), \quad (25)$$

with the eigenfunctions satisfying the BC given in equation (4).

More in detail, after solving in section 3.1 the spectral problem of H_U , by determining its eigenfunctions in terms of the zeroes of a certain spectral function, in section 3.2 we compute the corresponding Wigner functions, and analyze some of their properties in the high-energy regime. Then, in section 3.3 we review the phase-space description of a classical particle in a box in order to compare the results.

3.1. Spectral problem

The eigenvalue equation (25) can be rewritten as the ordinary differential equation

$$\psi'' + \epsilon \psi = 0, \quad \epsilon = 2mE/\hbar^2 \in \mathbb{R}, \quad (26)$$

further supplied by the BC in equation (4). Here, ϵ represents the dimensionless energy. For $\epsilon \neq 0$, the eigenvalue equation (26) has a general solution of the form

$$\psi_U(x; \epsilon) = \frac{1}{N_U(k)} \left(C_U^+(k) e^{ikx} + C_U^-(k) e^{-ikx} \right), \quad x \in \left(-\frac{1}{2}, \frac{1}{2}\right), \quad (27)$$

where $C_U^\pm(k) \in \mathbb{C}$, $N_U(k) \in \mathbb{R}$ is a normalization constant, and

$$k := e^{i \arg(\epsilon)/2} \sqrt{|\epsilon|} \quad (28)$$

is the dimensionless wave number. Differently from ϵ which is always real, k can be either real or purely imaginary, respectively when $\epsilon \geq 0$ or $\epsilon < 0$. We recall that, in general, the eigenvalues of H_U accumulate to $+\infty$ and can be at most doubly degenerate (see e.g. Theorem 10.6.1 of [47]), thus depending on U there can be at most two vanishing eigenvalues $\epsilon = 0$. Moreover, the sum of the multiplicities of the negative eigenvalues is at most two [25, 45].

It is convenient to introduce the boundary values

$$\Psi_\pm := \Psi' \pm i\Psi = \begin{pmatrix} -\psi'\left(-\frac{1}{2}\right) \pm i\psi\left(-\frac{1}{2}\right) \\ +\psi'\left(\frac{1}{2}\right) \pm i\psi\left(\frac{1}{2}\right) \end{pmatrix}, \quad (29)$$

so that the BC in equation (4) can be compactly expressed as $\Psi_- = U\Psi_+$. After inserting the general solution $\psi_U(x; \epsilon)$, the above boundary values can be rewritten as

$$\Psi_{\pm} = \frac{1}{N_U} A_{\pm}(\epsilon) \begin{pmatrix} C_U^+(k) \\ C_U^-(k) \end{pmatrix}, \quad A_{\pm}(\epsilon) := \pm i \begin{pmatrix} (1 \mp k) e^{-ik/2} & (1 \pm k) e^{ik/2} \\ (1 \pm k) e^{ik/2} & (1 \mp k) e^{-ik/2} \end{pmatrix}. \quad (30)$$

Imposing the BC $\Psi_- = U\Psi_+$ is then equivalent to impose the homogeneous system

$$[A_-(\epsilon) - UA_+(\epsilon)] \begin{pmatrix} C_U^+(k) \\ C_U^-(k) \end{pmatrix} = 0, \quad (31)$$

whose non-trivial solutions are obtained by requiring that

$$F_U(\epsilon) := \det(A_-(\epsilon) - UA_+(\epsilon)) = 0. \quad (32)$$

In other words, the non-vanishing eigenvalues of H_U correspond to the real zeroes of the spectral function $F_U(\epsilon)$ ⁶. In terms of the parametrization (16), it is known [25, 27, 45] that, for $\epsilon \neq 0$,

$$F_U(\epsilon) = \sin(k) [k^2 (\cos(\eta) - m_0) + \cos(\eta) + m_0] - 2k [m_1 - \sin(\eta) \cos(k)], \quad (33)$$

with $k = e^{i \arg(\epsilon)/2} \sqrt{|\epsilon|}$ as in equation (28). As it turns out, the spectrum $\sigma(H_U)$ depends only on three of the four independent parameters characterizing the matrix $U \in U(2)$. Namely, it depends on η , m_0 and m_1 , which by now we call *spectral parameters*, but not on β , the *non-spectral parameter*. Seen as a manifold, the *spectral space*

$$\Sigma := [0, \pi] \times D \quad (34)$$

has the same structure of a (twisted) solid torus [45], see figure 4(a). In figure 4(b), as an example, we represent in Σ both Robin and pseudo-periodic conditions.

The zeroes of $F_U(\epsilon)$ can be found analytically only for some particular BCs. Nevertheless, as we will show, their asymptotic behavior in the high-energy regime $\epsilon \rightarrow +\infty$ follows a simple pattern. Since we are interested in the classical limit, that is in the high-energy regime, from now on we will focus only on the positive part of the spectrum:

$$\sigma_+(H_U) = \{E \in \sigma(H_U) : E > 0\}. \quad (35)$$

For the time being, let us denote with

$$(\epsilon_n(\eta, m_0, m_1))_{n \geq 1} \quad (36)$$

the sequence of the positive zeroes of $F_U(\epsilon)$ and with

$$k_n(\eta, m_0, m_1) := \sqrt{\epsilon_n(\eta, m_0, m_1)}, \quad n \geq 1, \quad (37)$$

the corresponding wave numbers, so that we have

$$\sigma_+(H_U) = \left\{ \frac{\hbar^2}{2m} k_n^2(\eta, m_0, m_1) : n \geq 1 \right\}. \quad (38)$$

⁶ We mention that the definition of the spectral function can be modified to account also for the zero eigenvalues, see [45] for details.

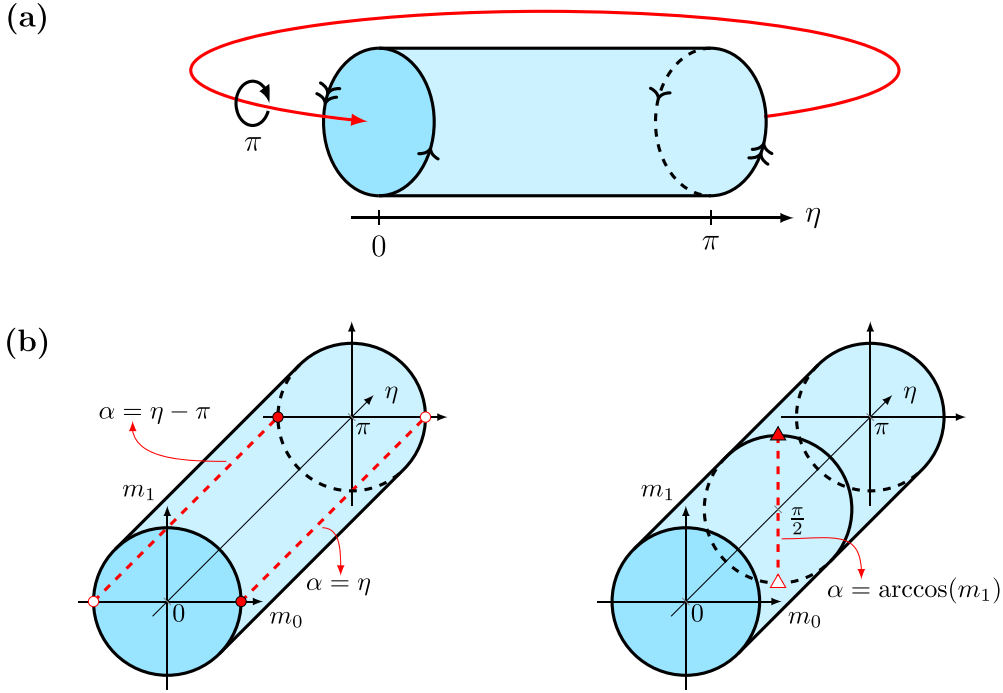


Figure 4. (a) The spectral space Σ can be constructed by gluing the two bases of the solid cylinder $[0, \pi] \times D$ after applying a global twist of angle π . The twist emerges as a consequence of the identification described by equation (13). (b) Some example of BCs depicted in the parameter space $[0, \pi] \times D$. Left: Robin conditions $\Psi' = -\cot(\frac{\alpha}{2})\Psi$ (red dashed lines), Neumann condition \circ and Dirichlet condition \bullet , see equation (17). Right: pseudo-periodic conditions $\psi(\frac{1}{2}) = e^{i\alpha}\psi(-\frac{1}{2})$ (red dashed line), periodic condition \blacktriangle and anti-periodic condition \blacktriangleleft , see equation (18).

To fix the expression of the eigenfunctions, we need to explicitly determine the coefficients $C_U^\pm(k)$ and the normalization $N_U(k)$. By using equation (31) we find

$$C_U^\pm(k) = \pm e^{\pm i\frac{k}{2}} \left[(1 \pm k)(m_0 + im_3) + (1 \mp k)(e^{-i\eta} + e^{\mp ik}(m_2 + im_1)) \right], \tag{39}$$

$$\begin{aligned} N_U^2(k) &= \int_{-\frac{1}{2}}^{\frac{1}{2}} |C_U^+(k)e^{ikx} + C_U^-(k)e^{-ikx}|^2 dx \\ &= |C_U^+(k)|^2 + |C_U^-(k)|^2 + 2\frac{\sin(k)}{k} \operatorname{Re} \left(C_U^+(k) \overline{C_U^-(k)} \right), \end{aligned} \tag{40}$$

where $m_2 = \sqrt{1 - m_0^2 - m_1^2} \cos(\beta)$ and $m_3 = \sqrt{1 - m_0^2 - m_1^2} \sin(\beta)$ as in equation (14). The above expressions reveal that, differently from the spectrum, the coefficients of the eigenfunctions in equation (27) do actually depend on the non-spectral parameter β . In conclusion, the function

$$\begin{aligned} \psi_{U,n}(x) &:= \psi_U(x; \epsilon_n(\eta, m_0, m_1)) \\ &= \frac{1}{N_{U,n}} \left(C_{U,n}^+ e^{ik_n(\eta, m_0, m_1)x} + C_{U,n}^- e^{-ik_n(\eta, m_0, m_1)x} \right), \end{aligned} \tag{41}$$

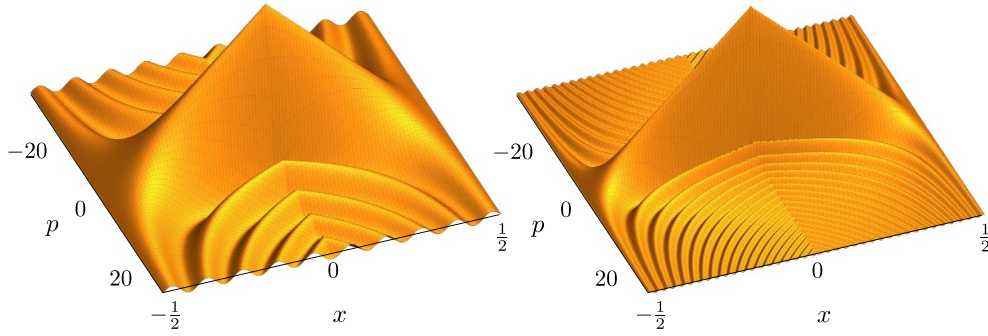


Figure 5. Plot of $\hbar f_{0,n}(x,p)$ for $\hbar = 1$ (left) and $\hbar = 1/4$ (right).

where $C_{U,n}^{\pm} := C_U^{\pm}(k_n(\eta, m_0, m_1))$ and $N_{U,n} := N_U(k_n(\eta, m_0, m_1))$, is a normalized eigenfunction of H_U corresponding to the eigenvalue $\hbar^2 \epsilon_n(\eta, m_0, m_1)/(2m)$. For later convenience let us observe that, in the expression (40) for the normalization $N_{U,n}$, the interference term proportional to $\sin(k_n(\eta, m_0, m_1))/k_n(\eta, m_0, m_1)$ is negligible for large n , thus we have

$$\lim_{n \rightarrow +\infty} \frac{|C_{U,n}^+|^2 + |C_{U,n}^-|^2}{N_{U,n}^2} = 1. \quad (42)$$

3.2. Classical limit of the Wigner functions

At this point we are ready to compute the Wigner function associated with an eigenfunction (41). Using the definition in equation (6) we obtain

$$W\psi_{U,n} = \frac{1}{N_{U,n}^2} \left[|C_{U,n}^+|^2 f_{1,n} + |C_{U,n}^-|^2 f_{-1,n} + 2 \operatorname{Re} \left(C_{U,n}^+ \overline{C_{U,n}^-} e^{2ik_n(\eta, m_0, m_1)x} \right) f_{0,n} \right], \quad (43)$$

where for each $s \in \{-1, 0, 1\}$:

$$f_{s,n}(x,p) := \frac{\Delta(x)}{\pi \hbar} \operatorname{sinc} \left(\frac{1}{\hbar} (p - s \hbar k_n) (1 - 2|x|) \right), \quad \forall x, p \in \mathbb{R}, \quad (44)$$

with the *triangular envelope* and the *sinc* functions being respectively given by

$$\Delta(y) := \chi(y) (1 - 2|y|), \quad \operatorname{sinc}(y) := \frac{\sin y}{y}, \quad \forall y \in \mathbb{R}. \quad (45)$$

A plot of $\hbar f_{0,n}(x,p)$ is given in figure 5.

The classical limit can be implemented by taking $n \rightarrow +\infty$, $\hbar \rightarrow 0$ so that $\hbar k_n(\eta, m_0, m_1)$ is kept fixed [4–6, 48–50]. Formally, it is obtained by setting

$$\hbar = \frac{p_c}{k_n(\eta, m_0, m_1)}, \quad (46)$$

where p_c is a reference value of the classical momentum, related to the classical reference energy E_c via

$$E_c = \frac{p_c^2}{2m}, \quad (47)$$

and by letting $n \rightarrow +\infty$.

By plugging equation (46) into equation (44), we get for all $s \in \{-1, 0, 1\}$:

$$f_{s,n}(x,p) = \frac{\Delta(x)k_n(\eta, m_0, m_1)}{\pi p_c} \operatorname{sinc}\left(\frac{k_n(\eta, m_0, m_1)}{p_c}(p - sp_c)(1 - 2|x|)\right), \quad \forall x, p \in \mathbb{R}. \quad (48)$$

Then, by using the well-know identity

$$\lim_{a \rightarrow 0} \frac{1}{\pi} \frac{\sin(x/a)}{x} = \lim_{a \rightarrow 0} \frac{1}{\pi a} \operatorname{sinc}\left(\frac{x}{a}\right) = \delta(x) \quad (49)$$

to be understood in the distributional sense, we obtain that

$$\lim_{n \rightarrow +\infty} f_{s,n}(x,p) = \chi(x) \delta(p - sp_c), \quad (50)$$

with $\delta(x)$ being the Dirac delta distribution. Moreover, by the Riemann-Lebesgue lemma [52] and by (42) one also gets

$$\frac{C_{U,n}^+ \overline{C_{U,n}^-}}{N_{U,n}^2} e^{2ik_n(\eta, m_0, m_1)x} \rightarrow 0 \quad (51)$$

in the distributional sense, as $n \rightarrow +\infty$. Therefore, as distributions,

$$\lim_{n \rightarrow +\infty} W\psi_{U,n}(x,p) - \chi(x) [\omega_{U,n} \delta(p - p_c) + (1 - \omega_{U,n}) \delta(p + p_c)] = 0,$$

where we introduced the shorthand

$$\omega_{U,n} = \frac{|C_{U,n}^+|^2}{N_{U,n}^2}, \quad (53)$$

and we used equation (42). Notice how, in the classical limit, the information regarding the quantum BCs is all contained in the coefficients $\omega_{U,n}$. If it happens that the sequence $(\omega_{U,n})_{n \geq 1}$ admits a limit, say

$$\lim_{n \rightarrow +\infty} \omega_{U,n} = \omega_U \in [0, 1], \quad (54)$$

then we also get a well-defined distributional limit for the Wigner function, that is,

$$W_U(x,p) := \lim_{n \rightarrow +\infty} W\psi_{U,n}(x,p) = \chi(x) [\omega_U \delta(p - p_c) + (1 - \omega_U) \delta(p + p_c)]. \quad (55)$$

As it turns out, the limit in equation (54) does not exist for all the BCs U . To determine the classical limit of the Wigner function, hence, we have to finely examine the asymptotic behavior of the coefficients $\omega_{U,n}$ in the high-energy regime, which in turn depends on the asymptotic behavior of the spectrum. We perform this analysis in section 4. Before proceeding, however, in the next subsection we suggest a classical interpretation of the limit Wigner function (55).

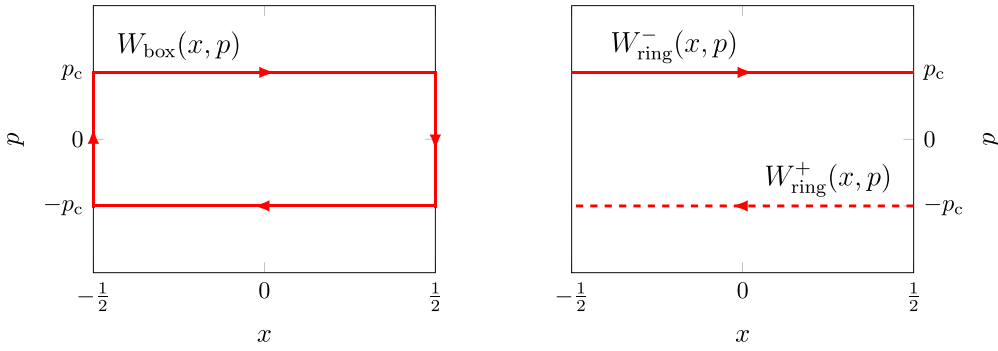


Figure 6. Joint probability distribution of a classical particle in a box (left) and in a ring (right); in the ring, the dashed (solid) line represents a (counter) clockwise motion.

3.3. Classical particle in a box

Let us briefly review the phase-space picture in the classical setting [18]. Heuristically, the joint (stationary) probability distribution of a classical particle of mass m and energy E_c which is confined in a box of unit length with elastically reflecting hard walls is given by

$$W_{\text{box}}(x, p) = \chi(x) \sqrt{2mE_c} \delta(p^2 - 2mE_c) \tag{56a}$$

$$= \frac{\chi(x)}{2} [\delta(p - p_c) + \delta(p + p_c)], \tag{56b}$$

where $p_c = \sqrt{2mE_c}$, and corresponds to a rectangular orbit in the phase-space, see the left panel of figure 6. If the particle is confined in a ring, instead, we can consider two classical orbits, associated with the joint probability distributions

$$W_{\text{ring}}^{\pm}(x, p) = \chi(x) \delta(p \mp p_c), \tag{57}$$

with $W_{\text{ring}}^+(x, p)$ and $W_{\text{ring}}^-(x, p)$ describing respectively a clockwise orbit and a counterclockwise one, see the right panel of figure 6.

Accordingly, the limit Wigner function $W_U(x, p)$ introduced in equation (55), when it exists, can be interpreted from a classical perspective in two different ways. Since

$$W_U(x, p) = \omega_U W_{\text{ring}}^+(x, p) + (1 - \omega_U) W_{\text{ring}}^-(x, p), \tag{58}$$

we can indeed consider $W_U(x, p)$ as the probability distribution of a classical ensemble of particles in a ring, of which a fraction ω_U is moving clockwise whereas the remaining fraction $1 - \omega_U$ is moving counterclockwise, see figure 7(a).

Another interesting interpretation is suggested by the ergodic theorem [53]: $W_U(x, p)$ can also represent the time-averaged probability distribution of a single classical particle in a ring with a junction, which acts as a door that can be opened or closed, allowing respectively the particle to pass through it or to be elastically reflected, thus inverting its motion, see figure 7(b). In particular, in order to implement the limit distribution $W_U(x, p)$, each time the particle approaches the junction, the door has to be closed (and then subsequently reopened) with probability ω_U if the particle is moving clockwise, and with probability $1 - \omega_U$ if it is moving counterclockwise. Notice however that, if the initial conditions are known, the probability distribution (58) can be also realized by a *deterministic* classical system.

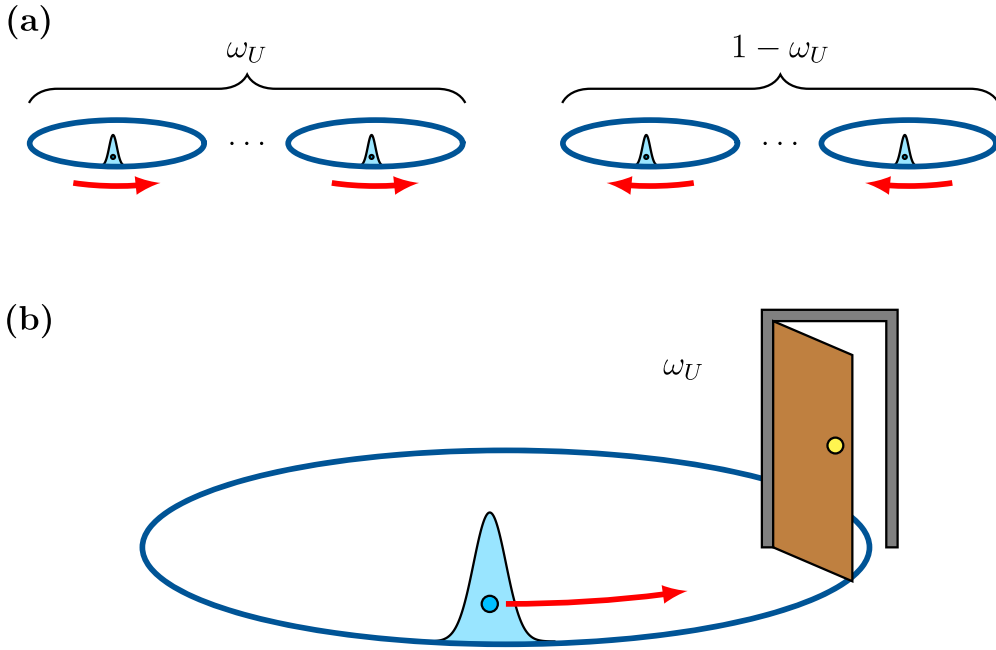


Figure 7. Two possible classical realization of the limit Wigner function $W_U(x, p)$: (a) statistical ensemble of particles in a ring; (b) time-average of a single particle in a ring with a door (a classical junction) which opens with probability ω_U .

4. Asymptotic analysis

In order to analyze the asymptotic behavior of the coefficients $\omega_{U,n}$ for large n , we start by observing that equation (39) implies that

$$|C_U^\pm(k)| = |kA_U^\pm(k) \pm B_U^\pm(k)|, \tag{59}$$

where

$$A_U^\pm(k) := m_0 + im_3 - e^{-i\eta} - e^{\mp ik}(m_2 + im_1), \tag{60a}$$

$$B_U^\pm(k) := m_0 + im_3 + e^{-i\eta} + e^{\mp ik}(m_2 + im_1). \tag{60b}$$

Notice that $A_U^\pm(k)$ can vanish, as it happens for example when $m_0 = \cos(\eta)$ and $m_3 = -\sin(\eta)$ (and thus $m_1 = m_2 = 0$). Therefore there are two possibilities for $\omega_{U,n}$, in the high-energy regime:

$$\lim_{n \rightarrow +\infty} \left(\omega_{U,n} - \frac{|A_{U,n}^+|^2}{|A_{U,n}^+|^2 + |A_{U,n}^-|^2} \right) = 0, \quad \text{if } A_{U,n}^\pm \neq 0, \tag{61a}$$

$$\lim_{n \rightarrow +\infty} \left(\omega_{U,n} - \frac{|B_{U,n}^+|^2}{|B_{U,n}^+|^2 + |B_{U,n}^-|^2} \right) = 0, \quad \text{if } A_{U,n}^\pm = 0, \tag{61b}$$

where $A_{U,n}^\pm := A_U^\pm(k_n(\eta, m_0, m_1))$, $B_{U,n}^\pm := B_U^\pm(k_n(\eta, m_0, m_1))$, and we used the fact that $k_n(\eta, m_0, m_1) \rightarrow +\infty$ for $n \rightarrow +\infty$.

We say that the sequence $(\omega_{U,n})_{n \geq 1}$ is *balanced*, when it admits the limit

$$\lim_{n \rightarrow +\infty} \omega_{U,n} = \frac{1}{2}, \tag{62}$$

and is *unbalanced* otherwise.

The balanced case can be easily characterized: equation (62) holds when

$$\lim_{n \rightarrow +\infty} \frac{|A_{U,n}^-|^2}{|A_{U,n}^+|^2} = 1, \quad \text{if } A_{U,n}^\pm \neq 0, \tag{63a}$$

$$\lim_{n \rightarrow +\infty} \frac{|B_{U,n}^-|^2}{|B_{U,n}^+|^2} = 1, \quad \text{if } A_{U,n}^\pm = 0. \tag{63b}$$

In turn, one can easily verify that these limits hold when one of the following sufficient conditions is satisfied.

(i) If $m_1 = 0$ and $m_2 = 0$, that is if we consider the asymmetric Robin BCs

$$U(\eta, \cos(\beta), 0, 0, \beta) = \begin{pmatrix} e^{i(\eta+\beta)} & 0 \\ 0 & e^{i(\eta-\beta)} \end{pmatrix}, \tag{64}$$

then $A_{U,n}^+ = A_{U,n}^-$ and $B_{U,n}^+ = B_{U,n}^-$ for each $n \geq 1$. Remarkably, these are the most general local BCs. Notice that they can be either regular (if e.g. $\beta = 0$, when they reduce to symmetric Robin BCs) and singular (if e.g. $\beta = -\eta \neq 0$, which gives a mixed Dirichlet-Robin BC).

(ii) If

$$\lim_{n \rightarrow +\infty} \sin(k_n(\eta, m_0, m_1)) = 0 \tag{65}$$

then $A_{U,n}^+ \sim A_{U,n}^-$ and $B_{U,n}^+ \sim B_{U,n}^-$ asymptotically as $n \rightarrow +\infty$. As we will show in the next subsection, this spectral condition is always satisfied for regular BCs.

On the other hand, the study of the unbalanced case is more involved, and it requires the asymptotic estimate of the spectral quantities $e^{\pm ik_n(\eta, m_0, m_1)}$ for large n . Thus, we devote section 4.1 to analyze in detail this spectral asymptotics. Then, in section 4.2, after gathering the obtained results, we finally classify the possible classical limits of the Wigner functions $W_{U,n}(x, p)$.

4.1. Spectral asymptotics

By defining the sequence

$$\delta_n(\eta, m_0, m_1) := k_n(\eta, m_0, m_1) - n\pi, \quad n \geq 1, \tag{66}$$

the spectral condition in equation (65), that is relevant for the balanced case, is equivalent to

$$\lim_{n \rightarrow +\infty} \sin(\delta_n(\eta, m_0, m_1)) = 0, \tag{67}$$

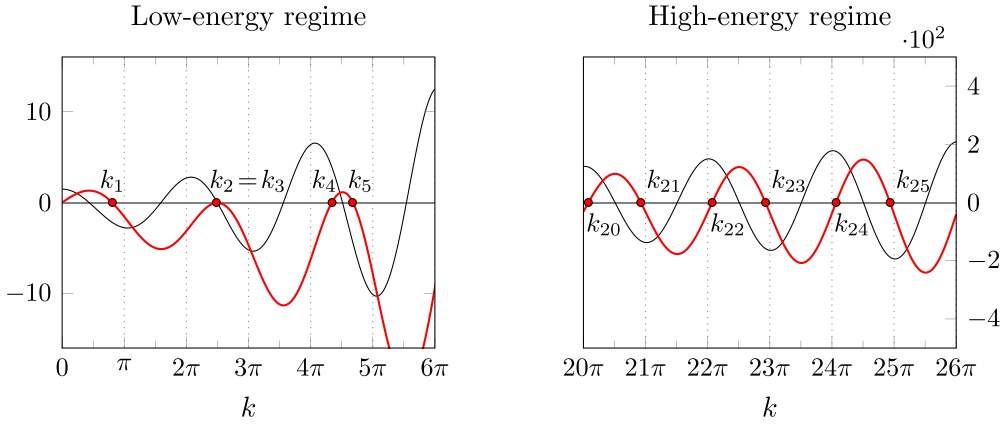


Figure 8. Plot of the spectral function $F_U(\sqrt{k})$ in equation (33) (red line) and of its derivative (black line) for the boundary condition $U(0, \cos \theta, \sin \theta, 0)$ with $\theta \approx 0.25$.

whereas the spectral quantities that are relevant for the unbalanced case can be rewritten as

$$e^{\mp i k_n(\eta, m_0, m_1)} = (-1)^n e^{\mp i \delta_n(\eta, m_0, m_1)}. \quad (68)$$

As it turns out, the behavior of $(\delta_n(\eta, m_0, m_1))_{n \geq 1}$ can be quite erratic for small values of n , but becomes more regular for large n , see figure 8 for an example. The currently available spectral estimates associated with the Weyl law for quantum graphs [54, 55] are not enough to characterize the remainder term in equation (66), as they just imply that $\delta_n(\eta, m_0, m_1) = o(n)$, for the system under study (which can be regarded as the ‘building block’ of more complex quantum graphs). However, in the particular situation considered here, the asymptotic behavior of δ_n is known, see section 1.5 of [56]. In this subsection we thus determine, on the lines of [56], the asymptotics of $\delta_n(\eta, m_0, m_1)$ needed to analyze the limit of the coefficients $\omega_{U,n}$.

To achieve this, let us rewrite the spectral function as

$$F_U(\epsilon) = a_U(k) k^2 + b_U(k) k + c_U(k), \quad \epsilon > 0, \quad (69)$$

where $k = \sqrt{\epsilon}$ and

$$a_U(k) := \sin(k) (\cos(\eta) - m_0), \quad (70a)$$

$$b_U(k) := -2(m_1 - \sin(\eta) \cos(k)), \quad (70b)$$

$$c_U(k) := \sin(k) (\cos(\eta) + m_0). \quad (70c)$$

It is convenient to separate the analysis into three cases:

- BCs U such that $k_n(\eta, m_0, m_1) = n\pi$ and hence $a_U(k_n(\eta, m_0, m_1)) = 0$ for all $n \geq 1$ (exact cases including Dirichlet BCs);
- BCs U such that $\cos \eta = m_0 \neq 1$ and hence $a_U(k) = 0$ for all $k > 0$ (singular BCs);
- all the remaining BCs U (regular BCs).

4.1.1. *Exact cases.* We first consider the case of BCs $U = U(\eta, m_0, m_1, \beta)$ such that $k_n(\eta, m_0, m_1) = n\pi$ for all $n \geq 1$. We show that this case occurs if and only if $\eta = m_1 = 0$. In fact,

$$F_U\left((2n\pi)^2\right) = -4n\pi[m_1 - \sin(\eta)] = 0 \Leftrightarrow m_1 = \sin(\eta), \tag{71}$$

and

$$F_U\left((2n+1)^2\pi^2\right) = -2(2n+1)\pi[m_1 + \sin(\eta)] = 0 \Leftrightarrow m_1 = -\sin(\eta), \tag{72}$$

and hence $m_1 = \eta = 0$. In this case we have that for all $n \geq 1$:

$$\delta_n(0, m_0, 0) = 0, \tag{73}$$

which clearly implies the spectral condition (65). Notice that the corresponding BCs $U(0, m_0, 0, \beta)$ are always regular.

4.1.2. *Singular boundary conditions.* Let us now consider the singular BCs (22), i.e. $\cos(\eta) = m_0 \neq 1$. For this choice of parameters the spectral function simplifies to

$$F_U(\epsilon) = 2\sin(k)\cos(\eta) - 2k[m_1 - \sin(\eta)\cos(k)], \tag{74}$$

and by considering the equation

$$F_U\left(k_n(\eta, m_0, m_1)^2\right) = 0, \tag{75}$$

which, since $\eta \in (0, \pi)$, can be rearranged as

$$\cos(k_n(\eta, m_0, m_1)) - \frac{m_1}{\sin(\eta)} = -\frac{\cot(\eta)\sin(k_n(\eta, m_0, m_1))}{k_n(\eta, m_0, m_1)}, \tag{76}$$

we get

$$\left|\cos(k_n(\eta, m_0, m_1)) - \frac{m_1}{\sin(\eta)}\right| \leq \frac{\cot(\eta)}{k_n(\eta, m_0, m_1)}. \tag{77}$$

Notice that $|m_1/\sin(\eta)| \leq 1$. In this case, one can show [56] that for large n the sequence $(k_{2n-1}(\eta, m_0, m_1), k_{2n}(\eta, m_0, m_1))_{n \geq 1}$ is asymptotically close to the sequence

$$\left(2n\pi - \arccos\left(\frac{m_1}{\sin(\eta)}\right), 2n\pi + \arccos\left(\frac{m_1}{\sin(\eta)}\right)\right)_{n \geq 1}. \tag{78}$$

In our notations, since $\arccos(x) = \pi - \arccos(-x)$, we can restrict $\delta_n(\eta, m_0, m_1)$ to $[0, \pi]$ obtaining the asymptotic limits

$$\lim_{n \rightarrow +\infty} \delta_{2n}(\eta, \cos \eta, m_1) = \arccos\left(\frac{m_1}{\sin(\eta)}\right), \tag{79}$$

and

$$\lim_{n \rightarrow +\infty} \delta_{2n-1}(\eta, \cos \eta, m_1) = \arccos\left(-\frac{m_1}{\sin(\eta)}\right). \tag{80}$$

Remarkably, for $\eta = \pi/2$ we recover the exact spectral sequence [25], that is:

$$\delta_n \left(\frac{\pi}{2}, 0, m_1 \right) = \arccos \left((-1)^n m_1 \right). \tag{81}$$

For $m_1 = 0$, in particular, the correction is constant:

$$\delta_n \left(\frac{\pi}{2}, 0, 0 \right) = \frac{\pi}{2}. \tag{82}$$

Conversely, the limit $\eta \rightarrow 0$ (which gives Dirichlet BC) is ill-defined, and one should rely on the exact expression (73). We conclude that the asymptotic behavior of the sequence $(\delta_n(\eta, m_0, m_1))_{n \geq 1}$ for singular BCs has a residual dependence on U , and, for $m_1 \neq 0$, also on the parity $(-1)^n$ of n .

4.1.3. Regular boundary conditions. For what concerns the remaining (regular) BCs, we can now assume that $k \neq n\pi$, as the latter values have been discussed before. We rewrite the equation $F_U(\epsilon) = 0$ as

$$a_U(\epsilon) = \frac{b_U(\epsilon)}{k} + \frac{c_U(\epsilon)}{k^2}, \tag{83}$$

from which we get

$$\left| \sin(k) (\cos(\eta) - m_0) \right| = \left| \frac{-2(m_1 - \sin(\eta) \cos(k))}{k} + \frac{\sin(k) (\cos(\eta) + m_0)}{k^2} \right| \leq \left| \frac{6}{k} \right|. \tag{84}$$

Therefore for all $n \geq 1$:

$$\left| \sin(k_n(\eta, m_0, m_1)) \right| = \left| \sin(\delta_n(\eta, m_0, m_1)) \right| \leq \frac{6}{|\cos(\eta) - m_0|} \frac{1}{k_n(\eta, m_0, m_1)}. \tag{85}$$

Then, by using the fact that the wave numbers accumulate to $+\infty$, the above inequality implies the spectral condition in equation (65), that is

$$\lim_{n \rightarrow +\infty} \sin(\delta_n(\eta, m_0, m_1)) = 0. \tag{86}$$

4.1.4. Numerical results. To corroborate the asymptotic analysis, in figure 9 we plot the values of some wave numbers $k_n(\eta, m_0, m_1)$, which have been determined by numerically finding the zeroes of the spectral function, both in the low-energy regime (small n) and in the high-energy regime (large n), as function of the spectral parameters η, m_0, m_1 . The high-energy plots are consistent with the asymptotic formulas obtained so far. In figure 10 we also plot some exact values of $\omega_{U,n}$ in the high-energy regime, again as function of the spectral parameters η, m_0, m_1 . As expected, for $m_0 \neq \cos(\eta)$ (that is for regular BCs) we have that $\omega_{U,n} \approx 1/2$, while for $m_0 = \cos(\eta)$ we observe a residual dependence on U , and in particular on β .

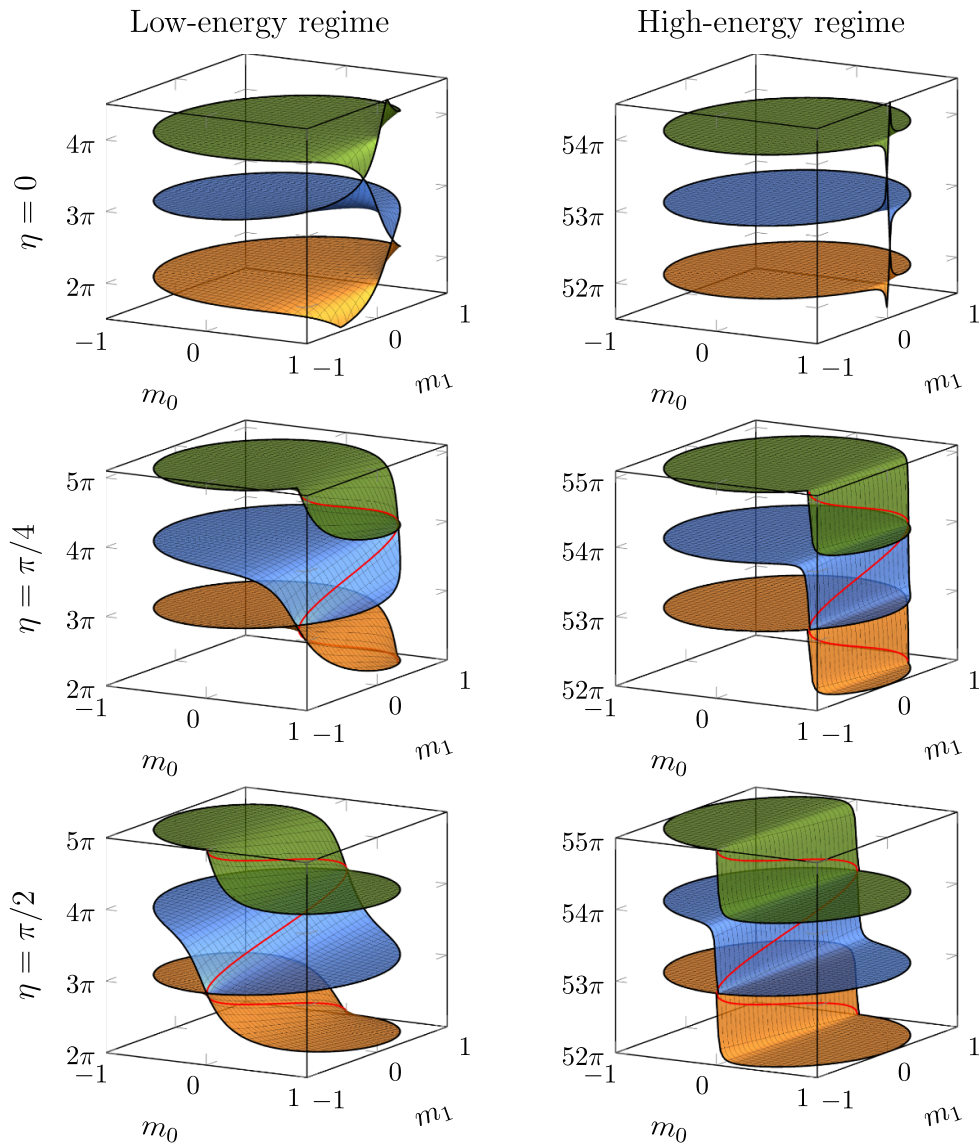


Figure 9. Exact values of some $k_n(\eta, m_0, m_1)$, plotted over the parameter space $(m_0, m_1) \in D$ for $\eta = 0$ (top row), $\eta = \frac{\pi}{4}$ (middle row) and $\eta = \frac{\pi}{2}$ (bottom row). For $\eta \neq 0$, red lines have been added representing the asymptotic formulae (79)–(80).

4.2. Asymptotics of the Wigner function

To sum up, we obtained two sufficient conditions for having a balanced classical limit. Indeed, we found that if U is a local BC, that is if $U = U(\eta, \cos(\beta), 0, 0, \beta)$ for $\eta \in [0, \pi)$ and $\beta \in [0, 2\pi)$, see equation (64), or if U is a regular BC, so that the spectral condition in equation (65)

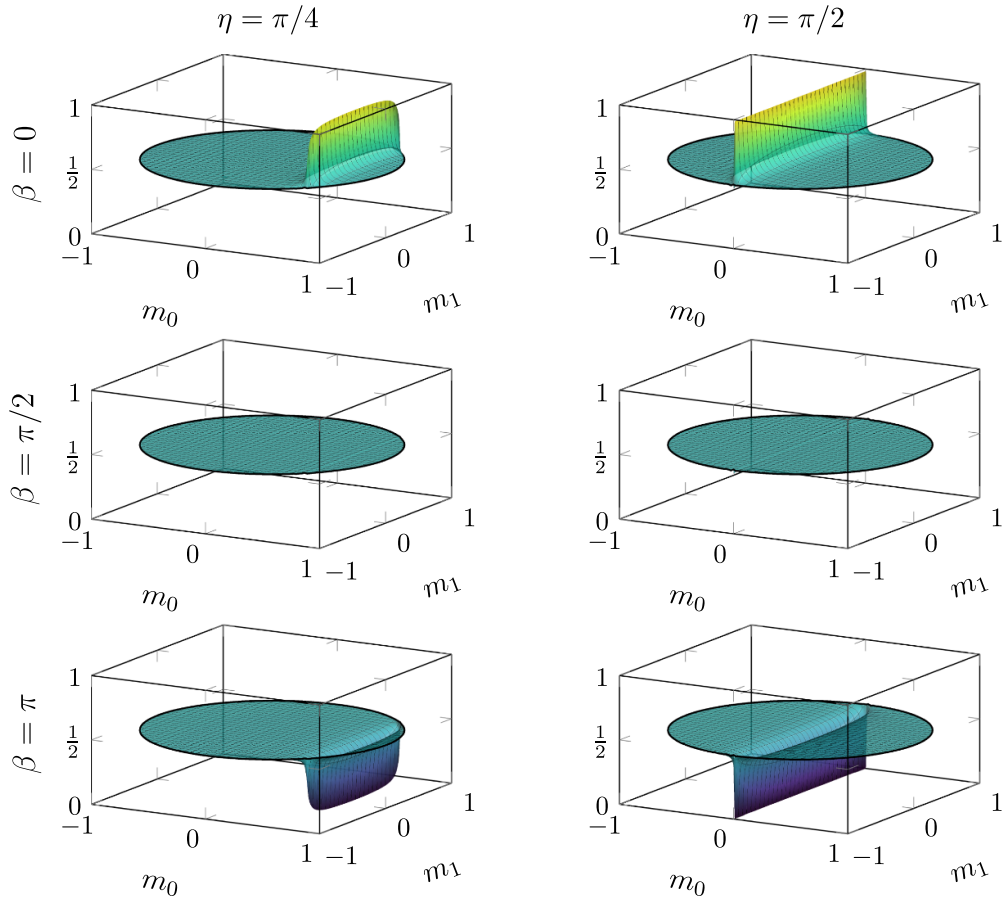


Figure 10. Exact values of $\omega_{U,52}$, plotted over the parameter space $(m_0, m_1) \in D$ for $\eta = \frac{\pi}{4}$ (left column) and $\eta = \frac{\pi}{2}$ (right column) and for different values of the non-spectral parameter β .

is satisfied [see equations (73) and (86)], then the coefficients $\omega_{U,n}$ have the well-defined high-energy limit

$$\omega_U = \lim_{n \rightarrow +\infty} \omega_{U,n} = \frac{1}{2}, \tag{87}$$

and the corresponding Wigner functions admit a limit in the form of equation (55) with balanced coefficients $\omega_U = 1 - \omega_U = 1/2$, that is:

$$\lim_{n \rightarrow +\infty} W\psi_{U,n}(x, p) = \frac{\chi(x)}{2} [\delta(p - p_c) + \delta(p + p_c)]. \tag{88}$$

This balanced classical limit is represented, respectively for the case of Dirichlet and Neumann BCs, in the first and in the second row of figure 11.

For singular *non-local* BCs, instead, the situation is complicated by the fact that even in the high-energy regime the correction $\delta_n(\eta, m_0, m_1)$ does generally still depend on the parity of n , see equations (79)–(80), thus not admitting a limit. However, since in the high-energy

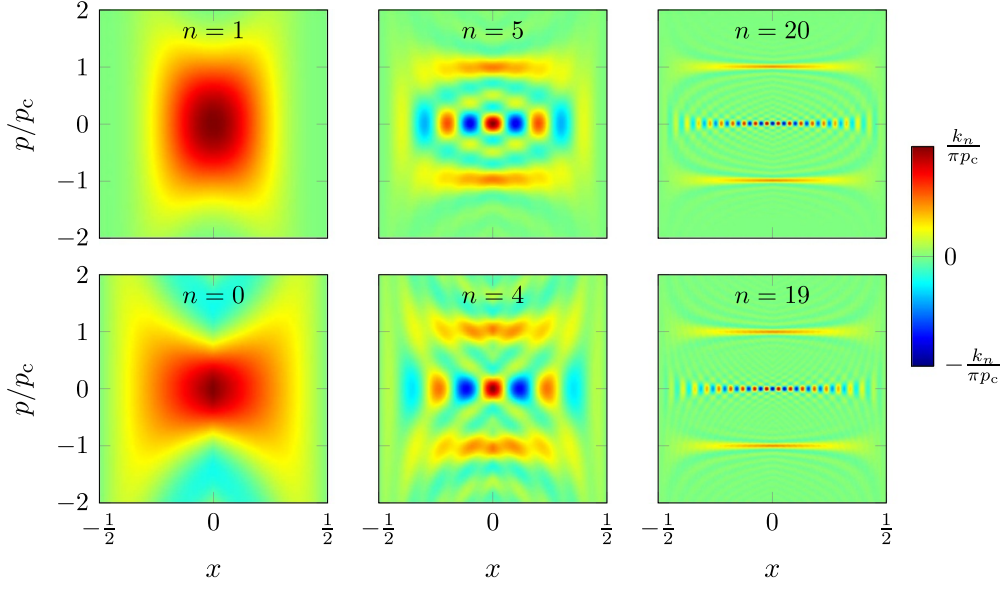


Figure 11. Density plot of $W\psi_{U,n}(x,p)$ for Dirichlet ($U=I$, first row) and Neumann ($U=-I$, second row) BCs; from left to right the value of n is increased, by setting $\hbar = p_c/k_n$, approaching the classical limit.

regime also the coefficients $\omega_{U,n}$ depend on n only through its parity, see equations (59)–(60) and (68), the following limits

$$\omega_{U,e} := \lim_{n \rightarrow +\infty} \omega_{U,2n}, \quad \omega_{U,o} := \lim_{n \rightarrow +\infty} \omega_{U,2n+1}, \quad (89)$$

are well-defined and finite. We stress that both $\omega_{U,2n}$ and $\omega_{U,2n+1}$ have a limit, but in general $\omega_{U,2n} \neq \omega_{U,2n+1}$. Accordingly, although for singular non-local BCs the Wigner functions $W\psi_{U,n}(x,p)$ do not generally admit a classical limit, the even and odd subsequences have the well-defined limits in the form of equation (55),

$$\begin{aligned} W_{U,e}(x,p) &:= \lim_{n \rightarrow +\infty} W\psi_{U,2n}(x,p) \\ &= \chi(x) [\omega_{U,e} \delta(p-p_c) + (1-\omega_{U,e}) \delta(p+p_c)], \end{aligned} \quad (90a)$$

$$\begin{aligned} W_{U,o}(x,p) &:= \lim_{n \rightarrow +\infty} W\psi_{U,2n+1}(x,p) \\ &= \chi(x) [\omega_{U,o} \delta(p-p_c) + (1-\omega_{U,o}) \delta(p+p_c)], \end{aligned} \quad (90b)$$

with (generally) unbalanced coefficients $\omega_{U,e} \neq 1/2$ and $\omega_{U,o} \neq 1/2$.

This phenomenon is shown in figure 12 for the family of ‘quasi-periodic’ BCs $U(\frac{\pi}{2}, 0, 0, \beta)$, given by

$$\psi\left(\frac{1}{2}\right) = i \cot\left(\frac{\beta}{2} + \frac{\pi}{4}\right) \psi\left(-\frac{1}{2}\right), \quad \psi'\left(\frac{1}{2}\right) = i \tan\left(\frac{\beta}{2} + \frac{\pi}{4}\right) \psi'\left(-\frac{1}{2}\right). \quad (91)$$

In particular, these BCs reduce for $\beta=0$ to the pseudo-periodic BC $U_{pp}(\pi/2)$, that is to $\psi(1/2) = i\psi(-1/2)$ and $\psi'(1/2) = i\psi'(-1/2)$, and to the mixed Dirichlet-Neumann BC

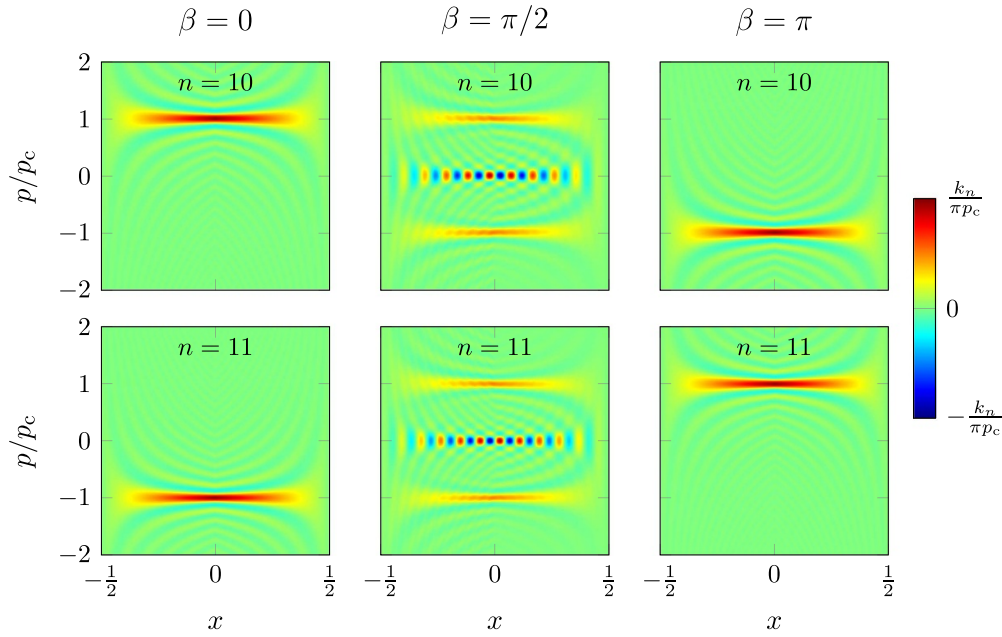


Figure 12. Density plot of $W\psi_{U,n}(x,p)$, with $\hbar = p_c/k_n$, for the singular BCs $U(\frac{\pi}{2}, 0, 0, \beta)$, with $n = 10$ (first row) and $n = 11$ (second row) and for different values of the non-spectral parameter β .

$\psi(1/2) = 0$ and $\psi'(-1/2) = 0$ for $\beta = \pi/2$. Remarkably, for any $\beta \in [0, 2\pi]$, by using equation (82) we are able to get the simple exact expression

$$\omega_{U(\frac{\pi}{2}, 0, 0, \beta), n} = \begin{cases} \cos\left(\frac{\beta}{2}\right)^2, & n \text{ even} \\ \sin\left(\frac{\beta}{2}\right)^2, & n \text{ odd} \end{cases}, \tag{92}$$

corresponding to the limit Wigner functions

$$W_{U(\frac{\pi}{2}, 0, 0, \beta), e}(x, p) = \chi(x) \left[\cos\left(\frac{\beta}{2}\right)^2 \delta(p - p_c) + \sin\left(\frac{\beta}{2}\right)^2 \delta(p + p_c) \right], \tag{93a}$$

$$W_{U(\frac{\pi}{2}, 0, 0, \beta), o}(x, p) = \chi(x) \left[\sin\left(\frac{\beta}{2}\right)^2 \delta(p - p_c) + \cos\left(\frac{\beta}{2}\right)^2 \delta(p + p_c) \right]. \tag{93b}$$

5. Discussion and outlook

We showed that in the classical limit both local boundary conditions and regular boundary conditions are associated with a ‘balanced’ ensemble, having a limit coefficient $\omega_U = 1/2$, so that the corresponding limit Wigner function coincides with the joint probability distribution of a classical particle in a box with elastically reflecting walls,

$$\lim_{n \rightarrow \infty} W\psi_{U,n}(x, p) = W_{\text{box}}(x, p). \tag{94}$$

Notice that in the limit any information about the quantum boundary condition is lost. In this sense, the whole family of quantum systems with local and regular boundary conditions correspond to one and the same classical system.

For what concerns singular non-local boundary conditions, the situation is more elaborate, as the coefficients $\omega_{U,n}$ do not generally admit a limit, but oscillate between the limits of the even and odd subsequences, that is between the values $\omega_{U,e}$ and $\omega_{U,o}$ defined in equation (89). The corresponding Wigner functions behave accordingly, with the even and odd subsequences having the limit Wigner functions $W_{U,e}(x,p)$ and $W_{U,o}(x,p)$ given by equations (90). These latter distributions have exactly the form (58), in general with an unbalanced coefficient $\omega_U \neq 1/2$ carrying a residual information—a classical echo—of the quantum boundary condition U . As we discussed in section 3.3, in this case, for a given parity, the limit Wigner function can be interpreted as the probability distribution of an ensemble of classical particles in a ring, with a fraction ω_U moving clockwise and a fraction $1 - \omega_U$ moving counterclockwise.

We conclude with some outlooks. In this Article we have analyzed the classical limit for the eigenfunctions of the non-relativistic kinetic-energy operator in a one-dimensional box with general self-adjoint boundary conditions. The corresponding classical distribution probabilities are stationary, i.e. time-independent. Performing a similar analysis by considering suitable *wave packets*, instead of the eigenfunctions, we expect to obtain a different classical distribution [18, 57] mimicking a classical dynamical orbit. Future research will be devoted to this subject. Besides, more generally, it is still an open question if in the classical limit different self-adjoint extensions of a given operator all collapse (in a suitable sense) to the same classical object. One could investigate this problem by looking at the asymptotic behavior of the symbols associated with the different self-adjoint extensions of the operator [50, 51]. Other interesting generalizations of the present work may involve the analysis of a particle with spin and of a relativistic particle in a box (with general boundary conditions) [58–60], as well as the case of multiple particles [61].

Data availability statement

The data that support the findings of this study are available upon reasonable request from the authors.

Acknowledgments

This work was partially supported by Istituto Nazionale di Fisica Nucleare (INFN) through the Project ‘QUANTUM’, by PNRR MUR Project PE0000023-NQSTI, by Regione Puglia and QuantERA ERA-NET Cofund in Quantum Technologies (Grant No. 731473), Project PACE-IN, by the Italian National Group of Mathematical Physics (GNFM-INdAM), and by the Italian funding within the ‘Budget MUR—Dipartimenti di Eccellenza 2023–2027’ - Quantum Sensing and Modelling for One-Health (QuaSiModO).

ORCID iDs

Giuliano Angelone  <https://orcid.org/0000-0002-0733-3380>
Paolo Facchi  <https://orcid.org/0000-0001-9152-6515>

References

- [1] Wigner E 1932 On the quantum correction for thermodynamic equilibrium *Phys. Rev.* **40** 749–59
- [2] Hillery M, O’Connell R F, Scully M O and Wigner E P 1984 Distribution functions in physics: Fundamentals *Phys. Rep.* **106** 121–67
- [3] Lee H-W 1995 Theory and application of the quantum phase-space distribution functions *Phys. Rep.* **259** 147–211
- [4] Cabrera G G and Kiwi M 1987 Large quantum-number states and the correspondence principle *Phys. Rev. A* **36** 2995–8
- [5] Hassoun G Q and Kobe D H 1989 Synthesis of the Planck and Bohr formulations of the correspondence principle *Am. J. Phys.* **57** 658–62
- [6] Man’ko V I, Marmo G, Simoni A, Stern A and Ventriglia F 2005 Tomograms in the quantum-classical transition *Phys. Lett. A* **343** 251–66
- [7] Koczor B, Zeier R and Glaser S J 2020 Continuous phase-space representations for finite-dimensional quantum states and their tomography *Phys. Rev. A* **101** 022318
- [8] Przanowski M, Brzykcy P and Tosiek J 2014 From the Weyl quantization of a particle on the circle to number-phase Wigner functions *Ann. Phys.* **351** 919–34
- [9] Kowalski K and Ławniczak K 2021 Wigner functions and coherent states for the quantum mechanics on a circle *J. Phys. A: Math. Theory* **54** 275302
- [10] Zhang S and Vourdas A 2003 Phase space methods for particles on a circle *J. Math. Phys.* **44** 5084
- [11] Rigas I, Sánchez-Soto L L, Klimov A B, Řeháček J and Hradil Z 2011 Orbital angular momentum in phase space *Ann. Phys.* **326** 426–39
- [12] Ligabò M 2016 Torus as phase space: Weyl quantization, dequantization and Wigner formalism *J. Math. Phys.* **57** 082110
- [13] Dias N C Prata J N 2002 Wigner functions with boundaries *J. Math. Phys.* **43** 4602
- [14] Kryukov S and Walton M A 2005 On infinite walls in deformation quantization *Ann. Phys.* **317** 474–91
- [15] Dias N C and Prata J N 2007 Deformation quantization of confined systems *Int. J. Quantum Inf.* **05** 257–63
- [16] Dias N C, Posilicano A and Prata J N 2011 Self-adjoint, globally defined Hamiltonian operators for systems with boundaries *Commun. Pure Appl. Math.* **10** 6
- [17] Casas M, Krivine H and Martorell J 1991 On the Wigner transforms of some simple systems and their semiclassical interpretation *Eur. J. Phys.* **12** 105
- [18] Belloni M, Doncheski M A and Robinett R W 2004 Wigner quasi-probability distribution for the infinite square well: energy eigenstates and time-dependent wave packets *Am. J. Phys.* **72** 1183–92
- [19] Walton M A 2007 Wigner functions, contact interactions and matching *Ann. Phys.* **322** 2233–48
- [20] Al-Hashimi M H and Wiese U-J 2021 Canonical quantization on the half-line and in an interval based upon an alternative concept for the momentum in a space with boundaries *Phys. Rev. Res.* **3** 033079
- [21] Robinett R W 1995 Quantum and classical probability distributions for position and momentum *Am. J. Phys.* **63** 823–32
- [22] Robinett R W 2002 Visualizing classical and quantum probability densities for momentum using variations on familiar one-dimensional potentials *Eur. J. Phys.* **23** 165
- [23] Bernal J, Martín-Ruiz A and García-Melgarejo J 2013 A simple mathematical formulation of the correspondence principle *J. Mod. Phys.* **4** 108–12
- [24] Teschl G 2014 Mathematical methods in quantum mechanics *Graduate Studies in Mathematics, American Mathematical Society*
- [25] Bonneau G, Faraut J and Valent G 2001 Self-adjoint extensions of operators and the teaching of quantum mechanics *Am. J. Phys.* **69** 322–31
- [26] Asorey M, Ibort A and Marmo G 2005 Global theory of quantum boundary conditions and topology change *Int. J. Mod. Phys. A* **20** 1001–25
- [27] Asorey M, Ibort A and Marmo G 2015 The topology and geometry of self-adjoint and elliptic boundary conditions for Dirac and Laplace operators *Int. J. Geom. Methods Mod. Phys.* **12** 06
- [28] Ibort A, Lledó F and Pérez-Pardo J M 2015 Self-adjoint extensions of the Laplace-Beltrami operator and unitaries at the boundary *J. Funct. Anal.* **268** 634–70
- [29] Facchi P, Garnerò G and Ligabò M 2018 Self-adjoint extensions and unitary operators on the boundary *Lett. Math. Phys.* **108** 195–212

- [30] Case W B 2008 Wigner functions and Weyl transforms for pedestrians *Am. J. Phys.* **76** 937–46
- [31] Facchi P, Garnero G and Ligabò M 2018 Quantum cavities with alternating boundary conditions *J. Phys. A: Math. Theory* **51** 105301
- [32] Belchev B and Walton M A 2010 On Robin boundary conditions and the Morse potential in quantum mechanics *J. Phys. A: Math. Theory* **43** 085301
- [33] Kurasov P 1996 Distribution Theory for Discontinuous Test Functions and Differential Operators with Generalized Coefficients *J. Math. Anal. Appl.* **201** 297
- [34] Exner P and Grosse H 1999 Some properties of the one-dimensional generalized point interactions (a torso) (arXiv:math-ph/9910029)
- [35] Albeverio S and Kurasov P 2000 *Singular Perturbations of Differential Operators* (Cambridge University Press)
- [36] Tsutsui I, Fülöp T and Cheon T 2001 Möbius structure of the spectral space of Schrödinger operators with point interaction *J. Math. Phys.* **42** 5687–97
- [37] Gnuzmann S and Smilansky U 2006 Quantum graphs: Applications to quantum chaos and universal spectral statistics *Adv. Phys.* **55** 527–625
- [38] Gadella M, Negro J and Nieto L M 2009 Bound states and scattering coefficients of the $-a\delta(x) + b\delta'(x)$ potential *Phys. Lett. A* **373** 1310–3
- [39] Balachandran A, Bimonte G, Marmo G and Simoni A 1995 Topology change and quantum physics *Nucl. Phys. B* **446** 299–314
- [40] Shapere A D, Wilczek F and Xiong Z 2012 Models of topology change 2012 (arXiv:1210.3545 [hep-th])
- [41] Asorey M, Facchi P, Marmo G and Pascazio S 2013 A dynamical composition law for boundary conditions *J. Phys. A: Math. Theory* **46** 102001
- [42] Facchi P, Garnero G, Marmo G, Samuel J and Sinha S 2018 Boundaries without boundaries *Ann. Phys.* **394** 139–54
- [43] Di Martino S, Anzà F, Facchi P, Kossakowski A, Marmo G, Messina A, Militello B and Pascazio S 2013 A quantum particle in a box with moving walls *J. Phys. A: Math. Theor.* **46** 365301
- [44] Di Martino S and Facchi P 2015 Quantum systems with time-dependent boundaries *Int. J. Geom. Methods Mod. Phys.* **12** 1560003
- [45] Angelone G, Facchi P and Marmo G 2022 Hearing the shape of a quantum boundary conditions *Mod. Phys. Lett. A* **37** 2250114
- [46] Lange R-J 2015 Distribution theory for Schrödinger’s integral equation *J. Math. Phys.* **56** 122105
- [47] Zettl A 2005 *Sturm-Liouville Theory (Mathematical Surveys and Monographs)* (American Mathematical Society)
- [48] Mostowski J and Pietraszewicz J 2021 Wigner function for harmonic oscillator and the classical limit (arXiv:2104.06638 [quant-ph])
- [49] Moretti V and van den Ven C J F 2022 The classical limit of Schrödinger operators in the framework of Berezin quantization and spontaneous symmetry breaking as an emergent phenomenon *Int. J. Geom. Methods Mod. Phys.* **19** 01
- [50] Cunden F D, Facchi P and Ligabò M 2023 The semiclassical limit of a quantum Zeno dynamics *Lett. Math. Phys.* **113** 114
- [51] Cunden F D, Ligabò M and Susca M C 2024 Truncated quantum observables and their semiclassical limit (arXiv:2404.15863 [math-ph])
- [52] Lighthill M J 1958 *An Introduction to Fourier Analysis and Generalised Functions* (Cambridge University Press)
- [53] Moore C C 2015 Ergodic theorem, ergodic theory and statistical mechanics *Proc. Natl Acad. Sci.* **112** 1907–11
- [54] Bolte J and Endres S 2009 The Trace Formula for Quantum Graphs with General Self Adjoint Boundary Conditions *Ann. Henri Poincaré* **10** 189–223
- [55] Odżak A and Śceta L 2019 On the Weyl Law for Quantum Graphs *Bull. Malays. Math. Sci. Soc.* **42** 119–31
- [56] Marchenko V A 1986 *Sturm-Liouville Operators and Applications* (Birkhäuser Basel)
- [57] Leubner C, Alber M and Schupfer N 1988 Critique and correction of the textbook comparison between classical and quantum harmonic oscillator probability densities *Am. J. Phys.* **56** 1123–9
- [58] Shin G R, Bialynicki-Birula I and Rafelski J 1992 Wigner function of relativistic spin-1/2 particles *Phys. Rev. A* **46** 645

- [59] Kowalski K and Rembieliński J 2016 The Wigner function in the relativistic quantum mechanics *Ann. Phys.* **375** 1–15
- [60] Angelone G 2023 Hearing the boundary conditions of the one-dimensional Dirac operator (arXiv:[2311.1756](https://arxiv.org/abs/2311.1756) [quant-ph])
- [61] De Bruyne B, Dean D S, Le Doussal P, Majumdar S N and Schehr G 2021 Wigner function for noninteracting fermions in hard-wall potentials *Phys. Rev. A* **104** 013314